LETTERS TO THE EDITOR

COMMENTS ON "SMART DIGITAL LOUDSPEAKER ARRAYS"*

I read with much interest Malcolm Hawksford's above paper[1] on the design and implementation of what he terms "micro drive unit" loudspeaker arrays, which provide constant-beamwidth sound radiation. The paper's FIR-filter-based design procedure for the driver transfer functions was very useful and informative, particularly given that the array can be designed to provide multiple beams of arbitrary size and direction. However, he analyzed only one type of array and did not provide any references to past work concerning the design of line arrays that provide broad-band constant-beamwidth radiation. No mention was made of other design methods [1]–[3] or other array types such as log arrays [4] or the so-called "constant-beamwidth transducer" (CBT) arrays [5]–[11], both of which provide wide-band constant-beamwidth acoustic output.

His extension of the design process to arrays that provide directional diffuse radiation is an important contribution. The three-dimensional display of the cross correlation between the on- and off-axis impulse responses is a very revealing measure of the coherence (or lack thereof) of the array's radiated sound field.

Hawksford's paper covered a wide range of topics, but my letter, although quite long, only contributes to the area of the design of constant-beamwidth arrays that provide forward-facing coherent beams. It would be interesting to apply Hawksford's stochastic design technique for generating incoherent diffuse radiation to the CBT array, but that is a topic for another study.

Although quite exhaustive, his coverage of the design of broad-band constant-beamwidth line arrays was limited to only one type, namely, constant-aperture linearly spaced straight-line arrays designed using a direct-synthesis method based on Fourier techniques. By constant aperture I mean that the acoustic length or aperture of the array is a constant number of wavelengths independent of frequency, so that the array provides constant-beamwidth operation. This means that the effective acoustic length of the array must decrease as the frequency increases. This is done by essentially driving fewer and fewer of the array's sources as the frequency increases.

In this letter I will outline a relatively simple alternate design method for the driver transfer functions for the constant-aperture constant-beamwidth line array type, and then present designs and polar simulation results for four line arrays: two of Hawksford's type designed using my alternate design method, and two designed using the CBT-style array type.

The first two arrays will be designed to provide two different beam shapes: 1) a wedge shape similar to the one provided by Hawksford's own design method, and 2) a rounded shape with lower sidelobes and improved off-axis behavior. The second set of two arrays both provide rounded beams: 1) a circularly curved CBT line array using frequency-independent shading [8], and 2) a straight-line delay-curved CBT array whose shading is also frequency independent, but in magnitude only [9]. It will be shown that the CBT-style arrays exhibit significantly less loss in their operating bands than the arrays analyzed by Hawksford, and in the case of the circularly curved CBT array they operate nearly an octave higher in frequency before grating lobes appear due to the finite spacing of the sources.

All the arrays were designed to meet Hawksford's specifications for his coherent-beam array example 2 [Hawksford,[1] p. 1144], that is, a single 45° wide beam aimed straight ahead, using 64 equally spaced point sources. The height of all the arrays was set to 1 m to encourage the formation of grating lobes below 20 kHz.

These arrays are then analyzed using the same techniques and presentation methods used by Hawksford:

- A cylindrical polar plot containing a composite plot of all the polars over a specific frequency range
- A three-dimensional polar plot of level versus angle versus linear frequency
- A three-dimensional array coefficient plot of coefficient magnitude versus element number versus linear frequency
- A three-dimensional plot of the cross correlation between the on- and off-axis impulse responses versus angle versus time.

All arrays were simulated at an observation distance of 250 m. Rotation was around either the array's center (for the straight-line arrays) or around the array's center of curvature (for the curved CBT arrays).

Alternate Design Method for Constant-Aperture Constant-Beamwidth Arrays

The design task is to determine the frequency response (possibly complex) of each source's processing channel so that the array generates a frequency-independent beam or beams with the proper characteristics, that is, with the proper shape, size (beamwidth), and steering direction.

The author's Fourier-transform-based direct-synthesis method essentially provides this information at a series of

*Manuscript received 2006 August 18; revised 2006 November 1.

[1]M. O. J. Hawksford, *J. Audio Eng. Soc.,* vol. 51, pp. 1133–1162 (2003 Dec.).

discrete design frequencies, which in turn can be interpolated to get finer frequency resolution. The end result of this process is that each channel has a frequency-dependent transfer function that is unique and different from the other channels and is based on a window shape that changes with frequency.

Here I will illustrate an alternate design method, which is also Fourier based. It starts with a time-domain-based window that sets the amplitude coefficients of the array sources (sometimes called shading) and then scales the window with frequency to achieve constant-beamwidth operation [3, sec. 3]. Rather than calculating a differently shaped window at each frequency, this scheme uses a constant-shape window whose width expands and contracts with frequency to force the line's acoustic length or aperture to be a constant number of wavelengths long, independent of frequency.

Once defined, the continuous time-domain-based window is used to set the strengths of the individual sources that make up the array by sampling the continuous window at the discrete source locations. The window width is then reduced as the frequency increases to maintain constant-beamwidth behavior of the array's radiated output. As the frequency increases and the window width is reduced, more and more of the array's outermost sources are simply shut off, leaving only the central sources to contribute to the acoustic output at the highest frequencies.

This progressive reduction of radiating sources as the frequency rises reduces the array's acoustic output by 6 dB for each doubling of frequency. The amount of reduction at each frequency is simply equal to the average value of the window that defines the array's source strengths at a particular frequency.

This alternate design method is outlined as follows:

1) Choose the line length L and the number of equally spaced sources N.

2) Define a continuous window function of position $w(x)$ over the interval $-0.5 \le x \le 0.5$, which is then mapped over the length of the array so that $x = \pm 0.5$ corresponds to $\pm L/2$, where L is the length of the array. This window defines the shape of the radiated beam. Typical time-domain windows used in signal processing [12] such as Gaussian, Hann, Kaiser–Bessel, or windowed-sinc functions may be used.

3) Define a window scaling function $F(x, f_N)$ that is a function of both position and frequency, which expands and contracts the window defined in step 2) as a function of frequency. This scaling function allows direct calculation of the frequency response for a particular source in the array. To simplify the frequency dependence, a normalized frequency f_N ($= f/f_L$) is defined, which is the ratio between frequency and the lower control frequency down to which constant-beamwidth operation is maintained. Note that $f_N \ge 1$ corresponds to the constant-beamwidth range. The scaling function defines the source strength at a particular position on the line at frequency f_N. Two forms of the scaling function are defined here, which are identical at and above $f_N = 1$.

Form 1,

$$F(x, f_N) = \begin{cases} w(x), & 0 \le f_N < 1 \\ w(f_N x), & f_N \ge 1. \end{cases} \quad (1)$$

Form 2,

$$F(x, f_N) = w(f_N x), \qquad f_N \ge 0. \quad (2)$$

For low frequencies below $f_N = 1$, form 1 [Eq. (1)] ceases expanding the window as the frequency is lowered and maintains a constant window shape, which completely covers the array. This form regularizes the transition between the beamwidth-control region ($f_N \ge 1$) and the low-frequency region ($f_N < 1$), and results in smoother off-axis behavior in the low-frequency region. Unfortunately this scaling function results in a fixed low-frequency loss equal to the average value of the window.

The form 2 scaling function [Eq. (2)] expands the window continually as the frequency is lowered and thus results in no low-frequency loss because the window essentially approaches a rectangular window at very low frequencies. Unfortunately the off-axis behavior of this form 2 function at low frequencies is not as well behaved as that of form 1 because of window truncation effects.

4) Sample the scaled and continuous window defined in step 3) at the positions of the sources to get the amplitude of a particular source as a function of frequency and position.

This array can then be steered by applying delays to each element of the array to effectively change the radiation angle of the array (not considered in this letter). When delays are applied, the real coefficients become complex.

Constant-Aperture Straight-Line Arrays

In this section two 1-m coherent constant-beamwidth constant-aperture straight-line arrays are designed and analyzed using the alternate design method. Both arrays contain 64 equally spaced point sources with a center-to-center spacing of 15.87 mm ($=$ 1000 mm/63). The first provides a wedge-shaped beam similar to the shape used by Hawksford in his design method, while the second provides a rounded more well-behaved beam.

Wedge-Shaped Beam Using a Tukey-Sinc Window

The Tukey-sinc window (my name for Hawksford's window) provides a wedge-shaped beam. It uses a sinc function rolled off on the ends with a raised-cosine function (a Tukey window [12]).

Tukey Window The Tukey window, which is defined over the interval $-0.5 \le x \le 0.5$, is given as

$$w_T(x, \alpha) = \begin{cases} 1, & |x| \le 0.5\alpha \\ 0.5 + 0.5 \cos\left[\dfrac{2\pi(|x| - 0.5\alpha)}{1 - \alpha}\right], & 0.5\alpha < |x| \le 0.5 \\ 0, & |x| > 0.5. \end{cases} \quad (3)$$

The parameter α defines the proportion of the total window covered by the raised-cosine function. The window changes smoothly from a purely raised-cosine window at $\alpha = 0$ to a rectangular window at $\alpha = 1$. A 15% taper ($\alpha = 0.85$) corresponds roughly to the cosine taper used by Hawksford [Hawksford,[1] eq. (11b)].

Tukey-Sinc Window The Tukey-sinc window is a sinc function windowed by a Tukey window and is given by the product of the two functions,

$$w_{TS}(x, \alpha, f_0) = w_T(x, \alpha)\mathrm{sinc}(2f_0x) = w_T(x, \alpha)\frac{\sin(2f_o\pi x)}{2f_0\pi x}. \quad (4)$$

The frequency parameter f_0 specifies the number of cycles of the sinc function contained within the window. Higher values of f_0 increase the sharpness of the edges of the radiated wedge-shaped beam.

Simulation and System Verification for Array Providing Wedge-Shaped Beam The alternate design method was used to design a constant-beamwidth array that provides a coherent wedge-shaped beam similar to Hawksford's polar example 2 (p. 1144), that is, a straight-facing beam of 45° beamwidth. An $\alpha = 0.85$ four-cycle ($f_0 = 4$) Tukey-sinc window [Eq. (4)] was chosen for this design. This window is shown in Fig. 1. Note that the window is zero for abs(x) > 0.5.

Fig. 2 shows the normalized far-field axial frequency response of this array for both the form 1 and the form 2 scaling functions using the Tukey-sinc window. This graph is a plot of the on-axis frequency response of the array as compared to the pressure that would be generated at the same observation point if all the array's sources were turned on and radiating with equal and in-phase levels. The 6-dB per octave rolloff at high frequencies is a direct result of the processing required for constant-beamwidth operation, which progressively shuts off more and more of the sources as frequency rises.

The Tukey-sinc window provides constant-beamwidth operation only above 3.5 kHz because of an inherent inefficiency. This inefficiency is due to the window's significantly low average value of only 0.122 (−18.3 dB), which results from of the narrowness of its main beam and its positive and negative undulations. Because of this, the form 2 scaling function [Eq. (2)] was chosen for this array to maximize the array's low- and mid-frequency output. Note that if the form 1 scaling function were chosen, the array's output below 3.5 kHz would be automatically attenuated by over 18 dB.

The axial level of the form 2 scaling falls at 6 dB per octave above 800 Hz and provides constant-beamwidth operation only above 3.5 kHz. Due to low window efficiency and the narrowness of the window's main lobe in relation to its total span, the array needs to be nearly 10 wavelengths long to generate a 45° beam. This is why the array exhibits constant-beamwidth behavior only above 3.5 kHz. The array designed in the next section uses a much more efficient window with a higher average value and wider main lobe to control the beamwidth down to a significantly lower frequency.

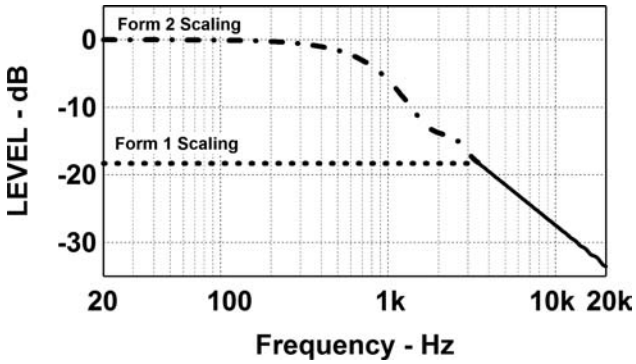

Fig. 2. Normalized far-field on-axis frequency response for constant-aperture constant-beamwidth straight-line array that provides a wedge-shaped beam. Array maintains constant-beamwidth operation only above 3.5 kHz (———) where response falls at 6 dB per octave. Form 1 scaling (•••) exhibits significant low-frequency loss (18.3 dB) compared to form 2 scaling (—•—).

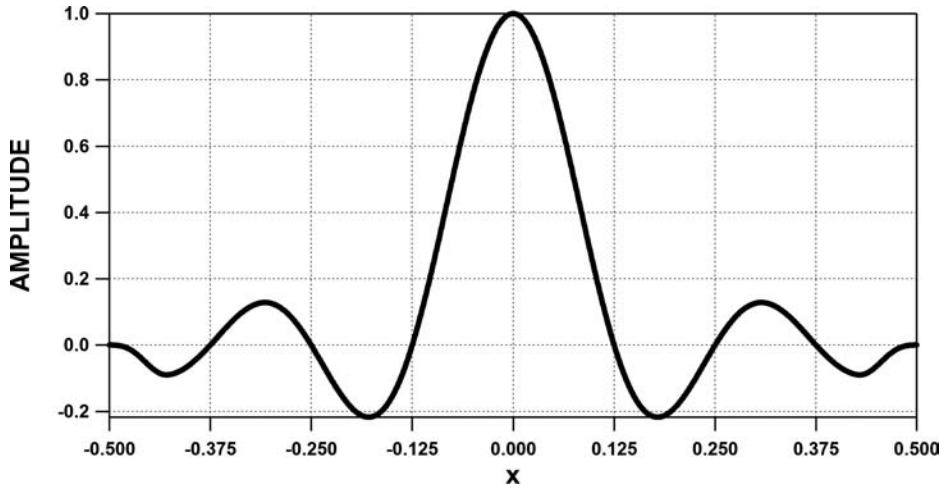

Fig. 1. Tukey-sinc window with $\alpha = 0.85$ and $f_0 = 4$ Hz used to design a constant-beamwidth straight-line array that provides a wedge-shaped beam.

Fig. 3 shows the array's cylindrical composite polar display. The display is composed of 501 polar curves drawn every 40 Hz from 0 to 20 kHz. All curves have been normalized to 0 dB at 0°. The wide lobes above 10 kHz, between 40° to 90° off the beam axis, are grating lobes due to the finite spacing of the sources.

To clarify the polar shape of the array in its beamwidth-control region, Fig. 4 shows a single polar at 6.3 kHz. Note the general wedge shape and the series of narrow off-axis lobes that commence at ±30° with levels that start at −20 dB and fall rapidly.

Fig. 5 shows the simulated three-dimensional polar plot of this array plotted versus a linear frequency scale from 0 to 20 kHz and a linear angular range of ±90°. The vertical scale is the magnitude of the polar plotted in dB referenced to the on-axis level. The array has been equalized flat on axis. The figure also includes a two-dimensional polar plot image projected on the bottom of the display. The lighter gray lines at the top of the display show the underside of the three-dimensional polar plot (true for all three-dimensional plots).

Note the polar ridges on the sides of the main beam which track the off-axis lobes (see Fig. 4). Also note the off-axis grating lobes that start to appear at about 10 kHz due to the finite spacing of the array sources. Hawksford predicts that spatial aliasing distortion will exist for frequencies higher than the half-wavelength spacing of the sources [Hawksford,[1] eq. (6)], or about 10.8 kHz in this instance.

Fig. 6 shows the array's three-dimensional coefficient plot versus frequency. The coefficients do not include the frequency-response equalization that makes the array flat on axis. Note that the plot basically takes the Tukey-sinc window of Fig. 1 and narrows it as the frequency increases. Note also how narrow the plot is at high frequencies, which implies that only a few sources are operating. At very low frequencies the window is expanded so that essentially all sources are operating equally. To minimize sampling errors, the coefficients have been shifted down by one-half element number so that the elements are aligned with the peaks of the Tukey-sinc window.

The array's three-dimensional cross-correlation plot between the on- and off-axis impulse responses is shown in Fig. 7. The plot displays the correlation over a time span of ±12.5 ms and ±90° of the array's main axis. This plot clearly shows the high on- and off-axis impulse correlation

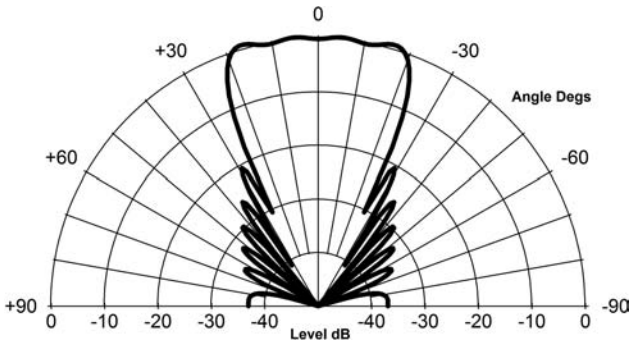

Fig. 4. Cylindrical polar plot at 6.3 kHz for constant-aperture constant-beamwidth array that provides a wedge-shaped beam.

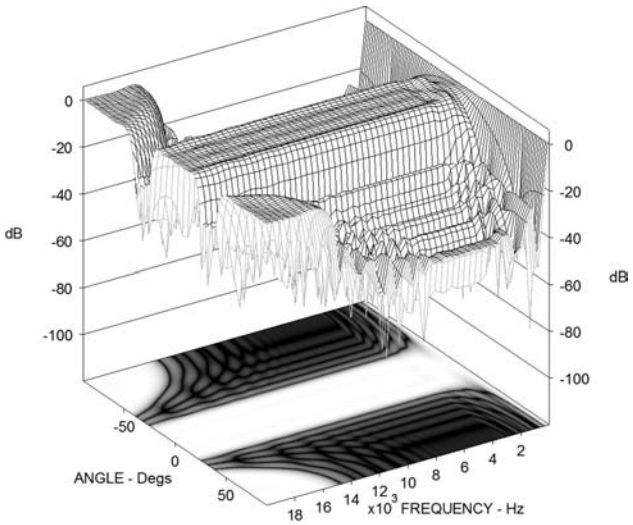

Fig. 5. Three-dimensional polar plot for constant-aperture constant-beamwidth array that provides a wedge-shaped beam. Bottom of display shows two-dimensional projected polar plot.

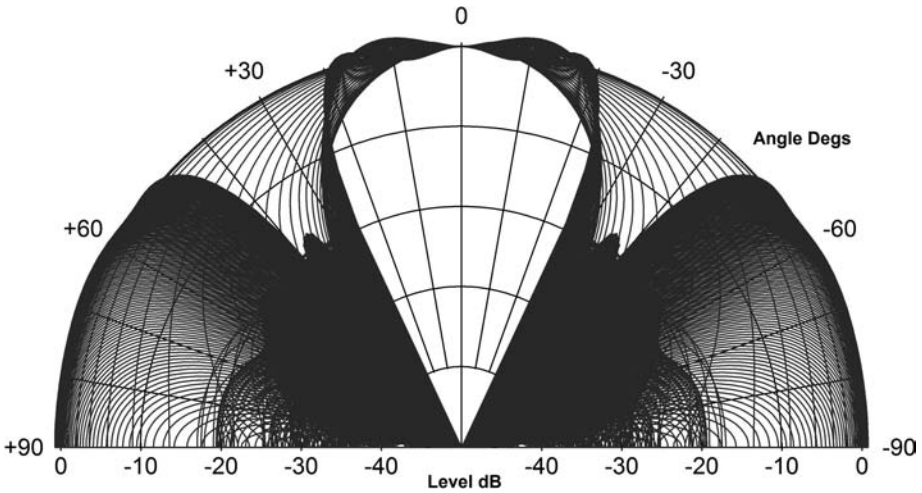

Fig. 3. Cylindrical composite polar plot for constant-beamwidth array that provides a wedge-shaped beam. Polar radial range is 50 dB with 10° angular increments.

in the array's rated 45° beam (±22.5° of the on-axis direction) at zero time.

Rounded-Shape Beam Using a Kaiser–Bessel Window

In this section a constant-aperture straight-line array is designed, which provides a coherent rounded-shape beam using the alternate design method. A Kaiser–Bessel window was chosen because it provides maximum level in its main beam while minimizing off-axis lobes.

Kaiser-Bessel Window The Kaiser–Bessel window [12] is defined as

$$w_{\mathrm{KB}}(x, \beta) = \begin{cases} \dfrac{I_0(\beta\sqrt{1-4x^2})}{I_0(\beta)}, & |x| \le 0.5 \\ 0, & |x| > 0.5 \end{cases} \tag{5}$$

where I_0 is the zero-order modified Bessel function of the first kind. The parameter β controls the sidelobe level in the frequency domain, with the sidelobe levels decreasing with increasing β. A value of $\beta = 6$ provides sidelobe levels that are down by about 45 dB whereas $\beta = 8$ provides sidelobes down by 60 dB.

Simulation and System Verification for Array Providing Rounded-Shape Beam The alternate design method will be used to design a constant-beamwidth array that provides a coherent rounded-shape beam of 45° beamwidth facing straight ahead. A $\beta = 6.34$ Kaiser–Bessel window was chosen for the design.

This window, shown in Fig. 8, exhibits a high average value of 0.487 (−6.2 dB), which is four times larger than the Tukey-sinc window used in the previous simulation. This allows the array to maintain constant-beamwidth operation a full two octaves below the previous design, drop-

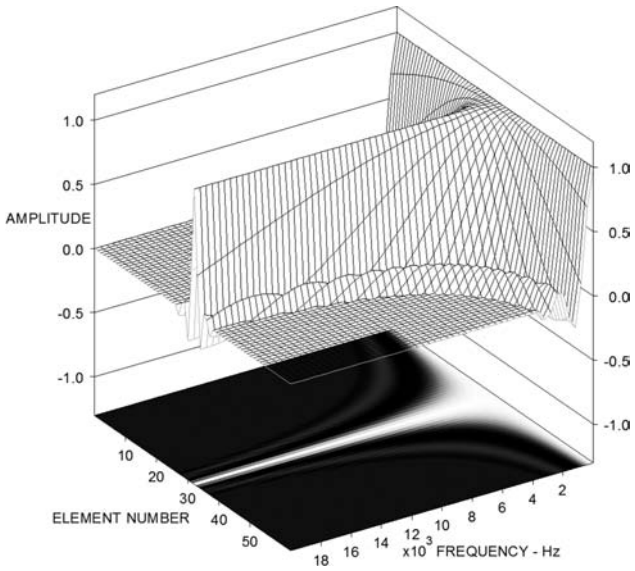

Fig. 6. Three-dimensional array coefficient plot versus frequency for constant-beamwidth array that provides a wedge-shaped beam. Bottom of display shows a two-dimensional projection of the three-dimensional plot. Note that coefficients do not include array's flat on-axis equalization.

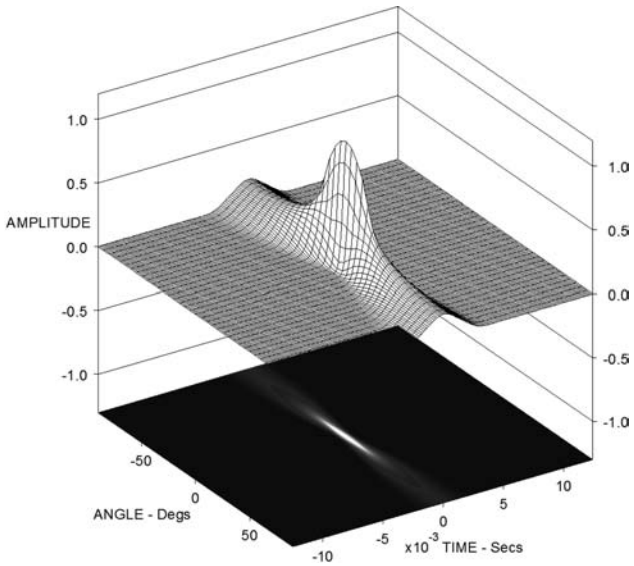

Fig. 7. Three-dimensional plot of cross correlation between on- and off-axis impulse responses for constant-beamwidth array that provides a wedge-shaped beam. Bottom of display shows a two-dimensional projection of the three-dimensional plot.

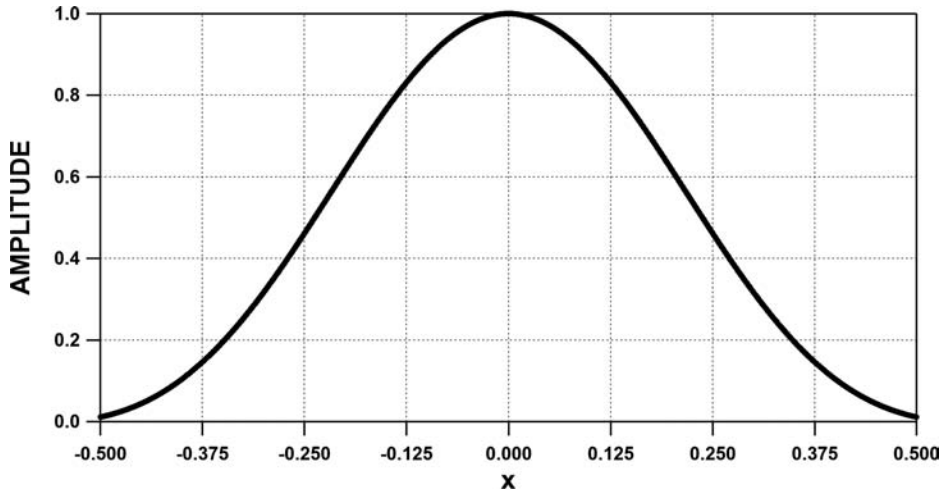

Fig. 8. Kaiser–Bessel window with $\beta = 6.34$ used to design a constant-beamwidth straight-line array that provides a rounded-shape beam.

ping from 3.48 kHz down to 870 Hz. In addition, the array now needs to be only 2.5 wavelengths long, rather than 10 wavelengths, to generate a constant 45° beamwidth.

Fig. 9 shows the normalized far-field axial frequency response of this array for both the form 1 and the form 2 windows as a function of frequency. Because the Kaiser–Bessel window exhibits significantly less axial loss than the previous array's window, I chose the higher attenuation form 1 scaling function [Eq. (1)] to implement the window frequency scaling. The form 1 scaling exhibits better polar control below the constant-beamwidth turnover point (870 Hz).

The array's cylindrical composite polar display is shown in Fig. 10. Note the uniformity of the polars between ±30°. The wide off-axis lobes between 35° and 90° off the beam's axis are grating lobes that appear above 10 kHz due to the finite spacing of the sources.

To clarify the polar shape of this array in its beamwidth-control region, Fig. 11 shows a single polar at 6.3 kHz. Note the rounded shape and the absence of sidelobes.

Fig. 12 shows the simulated three-dimensional polar plot of this array. As before, the array has been equalized flat on axis. The figure also includes a two-dimensional polar-plot image projected on the bottom of the display. Note the rounded appearance and extreme uniformity of the off-axis curves, between 800 Hz and 10 kHz, down to nearly 35 dB below the on-axis level. As before, note the off-axis grating lobes that start to appear at about 10 kHz due to the finite spacing of the array sources.

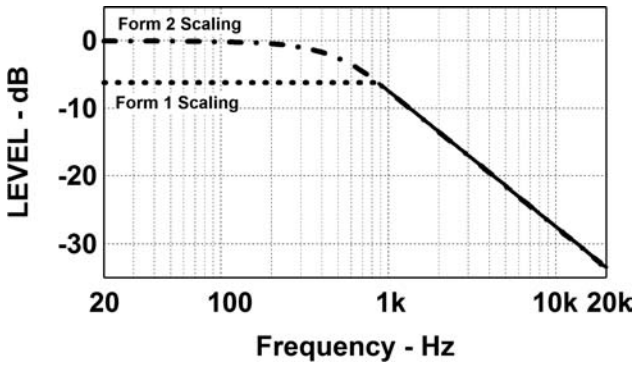

Fig. 9. Normalized far-field on-axis frequency response for constant-aperture constant-beamwidth straight-line array that provides a rounded-shape beam. Array maintains constant-beamwidth operation down to a relatively low 870 Hz (———). Form 1 scaling (•••) exhibits only 6.2-dB low-frequency loss compared to form 2 scaling (—•—).

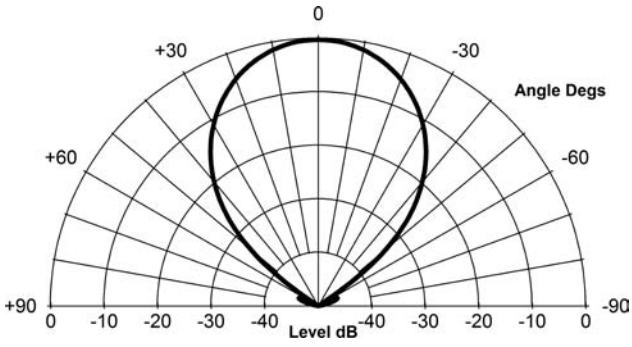

Fig. 11. Cylindrical polar plot at 6.3 kHz for constant-aperture constant-beamwidth array that provides a rounded-shape beam.

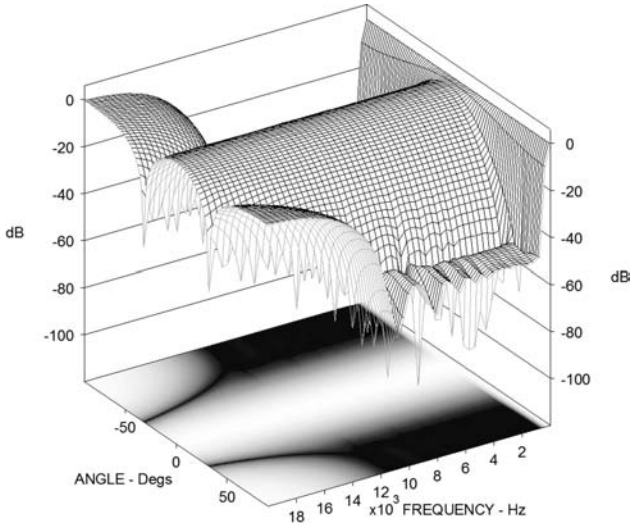

Fig. 12. Three-dimensional polar plot for constant-aperture constant-beamwidth array that provides a rounded-shape beam.

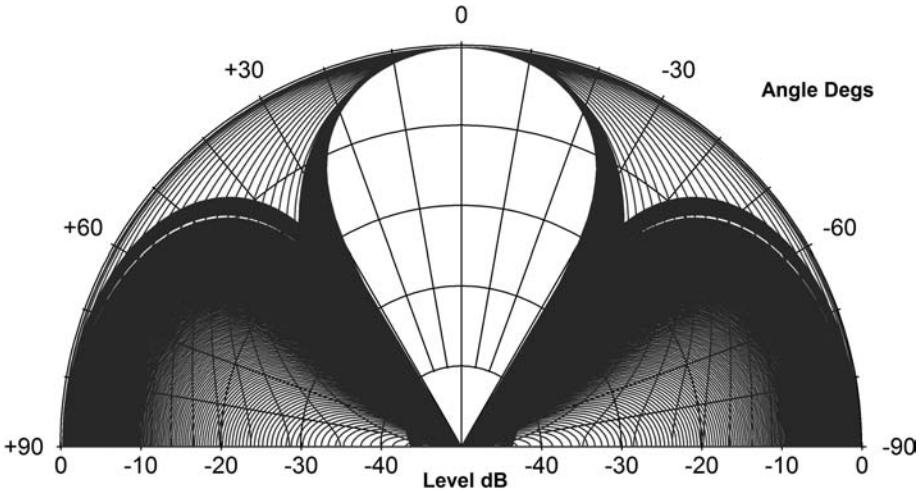

Fig. 10. Cylindrical composite polar plot for constant-beamwidth array that provides a rounded-shape beam. Polar radial range is 50 dB with 10° angular increments.

Fig. 13 shows the array's three-dimensional coefficient plot versus frequency. In contrast to the previous design (Fig. 6), at very low frequencies the window does not expand to fill all the sources with equal levels. This is due to the form 1 scaling chosen for the array. As before, the coefficients have been shifted down by one-half element number so that the elements are aligned with the peaks of the window.

Fig. 14 shows the array's three-dimensional cross-correlation plot between the on- and off-axis impulse responses. The plot displays the correlation over a time span of ±12.5 ms and ±90° of the array's main axis. This cross-correlation display is similar to the previous design, but the main lobe is slightly narrower in time.

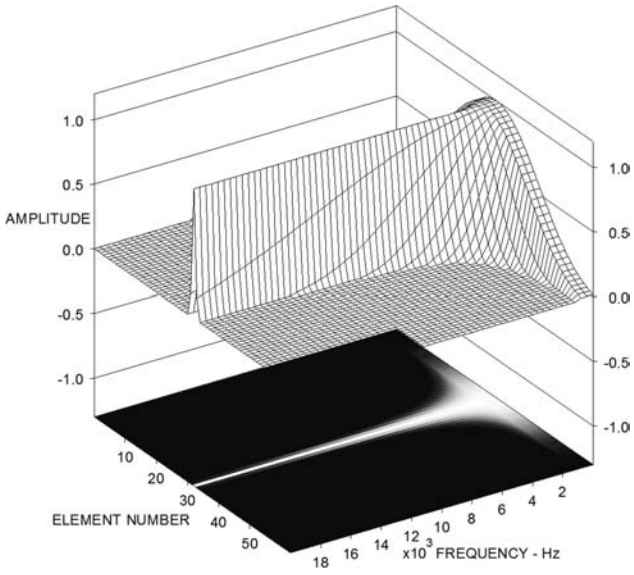

Fig. 13. Three-dimensional array coefficient plot versus frequency for constant-beamwidth array that provides a rounded-shape beam. Note that plot does not include array's flat on-axis equalization.

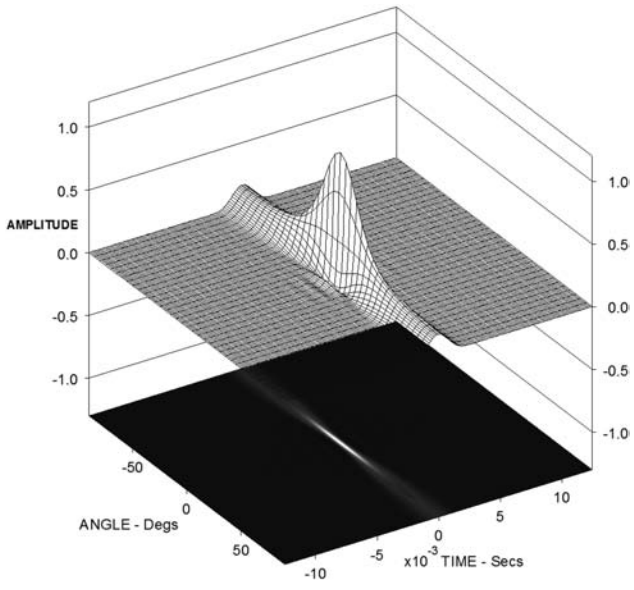

Fig. 14. Three-dimensional plot of cross correlation between on- and off-axis impulse responses for constant-aperture constant-beamwidth array that provides a rounded-shape beam.

Constant-Beamwidth Transducer (CBT) Arrays

Two CBT arrays of 1-m length are designed and analyzed in this section. The first is a circularly curved CBT array and the second is a straight-line delay-curved CBT array identical in physical configuration to the two previously analyzed arrays. Both arrays contain 64 equally spaced point sources.

CBT arrays are based on unclassified military underwater transducer research done in the late 1970s and early 1980s [1]–[3]. The research describes a curved-surface transducer in the form of a spherical cap with frequency-independent Legendre shading, which provides wide-band extremely constant beamwidth and directivity behavior with virtually no sidelobes. I applied the theory to circular-arc line arrays in 2000 [8] and extended the concept to straight-line arrays curved with the use of signal delays in 2002 [9]. I analyzed the sound field of CBT arrays in 2003 [10] and also showed the details of an experimental CBT curved-line array model in 2003 [11].

Note that physically curved CBT arrays cannot be steered easily by the use of delays as is the case with straight-line arrays. The physically curved CBT array can only be steered by circularly rotating the Legendre window function around a circular array, which includes many more sources than are required for a fixed-direction array. If steering is required, the straight-line delay-curved version of the CBT array is more appropriate.

Legendre Window

The CBT arrays are based on the use of a Legendre window, which can be approximated by a simplified four-term series approximation [8, eq. (3)],

$$U(x) \approx \begin{cases} 1 + 0.132|x| - 7.2|x|^2 + 5.944|x|^3, & |x| \le 0.5 \\ 0, & |x| > 0.5 \end{cases}$$

Here the Legendre approximation has been scaled by 2 and defined over the restricted $-0.5 \le x \le 0.5$ interval. This window is shown in Fig. 15 and has an average level of 0.619 (−4.2 dB), which is the highest level of any window used in this letter. Note that this window does not need to be frequency scaled because it is frequency independent, that is, it stays the same shape and covers the whole array at all frequencies. Effectively the curvature of the CBT array provides the frequency scaling that maintains constant-beamwidth operation.

Circularly Curved CBT Line Array Using a Frequency-Independent Legendre Window

The CBT design method was used to design a circularly curved constant-beamwidth array that provides a coherent rounded-shape beam of 45° beamwidth facing straight ahead. As before, the array is 1 m high, but contains 64 equally spaced point sources arrayed around a circular arc. Because the beamwidth (−6 dB) of a CBT array is approximately 64% of the wedge angle [8, fig. 10], the circular wedge has to be 70.3° (≈ 45°/0.64) to yield the proper beamwidth. The array then has a radius of curva-

ture of 0.868 m and a wedge circumference of 1.066 m. The source center-to-center spacing is 16.91 mm, which is about 6.6% greater than the spacing of the straight-line array.

Simulation and System Verification for Circularly Curved CBT Array Providing a Rounded-Shape Beam

Fig. 16 shows the normalized far-field on-axis frequency response of the CBT array. Note that the high-frequency rolloff of the CBT array is due to the curvature of the CBT array only, and not to a progressive depowering of the array sources as frequency rises, as in the previous constant-aperture arrays.

The array provides constant-beamwidth operation above 800 Hz, where the response falls at only 3 dB per octave. Compared to the two previous arrays where the response falls at 6 dB per octave, the CBT array provides much less high-frequency loss (nearly 12 dB less loss at 10 kHz compared to the previous arrays). As compared to the previous constant-aperture straight-line arrays, the lower high-frequency rolloff rate of the CBT array is a direct result of energizing a higher proportion of the sources at high frequencies. However, the CBT array has a fixed 4.2-dB low-frequency loss that cannot be avoided.

The CBT curved-line array's cylindrical composite polar display is shown in Fig. 17. Note the uniformity of the polars between ±35°. The wide lobes between 35° and 90° off the beam's axis are high-frequency grating lobes that start above 18 kHz due to the finite spacing of the sources.

To clarify the polar shape of this array in its beamwidth-control region, Fig. 18 shows a single polar at 6.3 kHz. As with the previous array, note the complete absence of sidelobes.

The three-dimensional polar plot of the CBT curved-line array is shown in Fig. 19. Note that the high-frequency grating lobes appear nearly an octave higher in frequency at 18 kHz than in previous arrays (of 10 kHz). This is primarily due to the curvature of the array randomizing the effective spacing of the sources. When the greater spacing of the CBT array sources is taken into account, the curved-line CBT array operates effectively up to the frequency where the center-to-center spacing of the sources is one wavelength [11, sec. 8.4]. This is in contrast to the straight-line arrays (the CBT straight-line array included), which only operate well up to the frequency where the center-to-center spacing of the sources is one-half wavelength.

Note also that the off-axis behavior of the CBT is not quite as uniform as that of the previous constant-aperture array shown in Fig. 12.

One major advantage of the circularly curved CBT array is that the directional pattern of the array is essentially independent of distance [5], [8]. I ran another three-dimensional polar plot of the CBT curved-line array at a close distance of 0.5 m in front of the array (not shown), and it was virtually the same as the three-dimensional polar plot run at 250 m (Fig. 19 here). Rotation in both cases was around the array's center of curvature.

Fig. 20 shows the array's three-dimensional coefficient plot versus frequency. Note that apart from the equalization that is applied to make the array flat on axis, the coefficients do not change with frequency. This is in contrast to the two previous designs, where the window narrows considerably with frequency to maintain constant-beamwidth operation. The physical curvature of the CBT

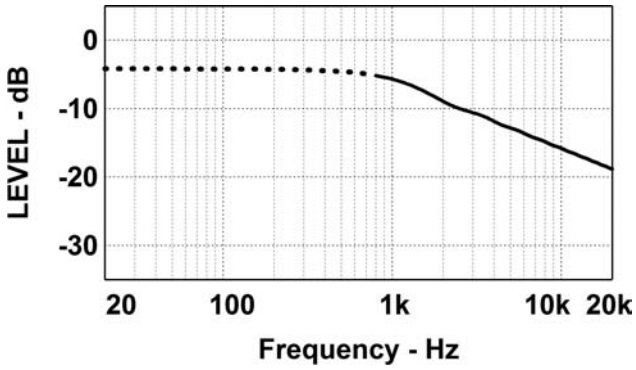

Fig. 16. Normalized far-field on-axis frequency response for circularly curved CBT constant-beamwidth array that provides a rounded-shape beam. Array maintains constant-beamwidth operation down to 800 Hz (———). The high-frequency power response of the CBT arrays rolls off at a rate of only 3 dB per octave, which is one-half of the 6 dB per octave rolloff rate of the previous constant-aperture arrays (Figs. 2 and 9).

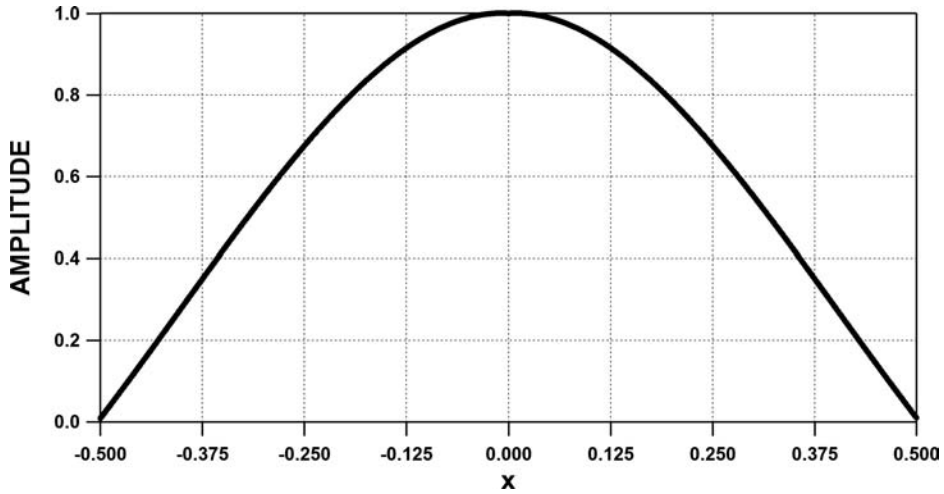

Fig. 15. Legendre window used to design a constant-beamwidth CBT array.

array automatically provides the constant-beamwidth operation.

The array's three-dimensional cross-correlation plot between the on- and off-axis impulse responses is shown in Fig. 21. The plot displays the correlation over a time span of ±12.5 ms and ±90° of the array's main axis. Note the time curvature of the plot, which reflects the physical curvature of the CBT array.

Straight-Line Delay-Curved CBT Line Array Using a Frequency-Independent Legendre Window

A straight-line array will also work as a physically curved CBT array if delay is used to effectively curve the array [9]. When this is done, the delay changes the array coefficients from real to complex and makes them frequency dependent. The magnitude of the coefficients is still equal to the Legendre window amplitude (Fig. 15) while their phase depends on the amount of delay and the frequency.

The straight-line delay-curved CBT design method is used in this section to design an array with the same specifications as before, that is, to provide a constant-beamwidth array that provides a coherent rounded-shape beam of 45° beamwidth facing straight ahead. The array configuration is identical to the constant-aperture arrays and includes 64 equally spaced sources arrayed on a 1-m straight line. Delays in each source's drive signal effectively create a 70° circular wedge.

Simulation and System Verification for Straight-Line CBT Array Providing a Rounded-Shape Beam The normalized axial frequency response of this array is essentially identical to the previous CBT array (Fig. 16) and is not repeated in this section.

Fig. 22 shows the straight-line delay-curved CBT array's cylindrical composite polar display. The main lobe is similar to that provided by the curved-line CBT array (Fig. 17), but the high-frequency grating lobes now commence at 10 kHz, the same as for the previous straight-line arrays.

To clarify the polar shape of this array in its beamwidth-control region, Fig. 23 shows a single polar at 6.3 kHz. The polar is similar to the curved-line CBT array's polar (Fig. 18) but exhibits less off-axis rejection for angles beyond 30°.

Fig. 24 shows the three-dimensional polar plot of this array. As compared to the curved-line CBT array plot

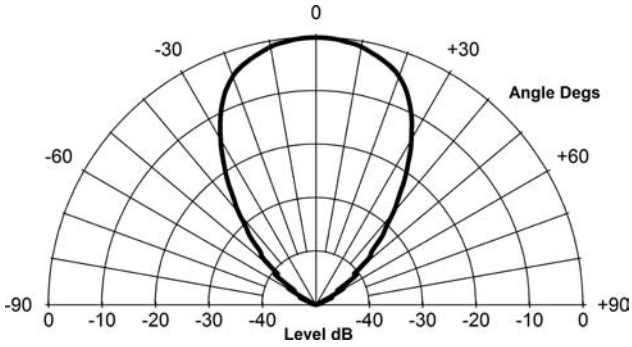

Fig. 18. Cylindrical polar plot at 6.3 kHz for CBT constant-beamwidth curved-line array that provides a rounded-shape beam.

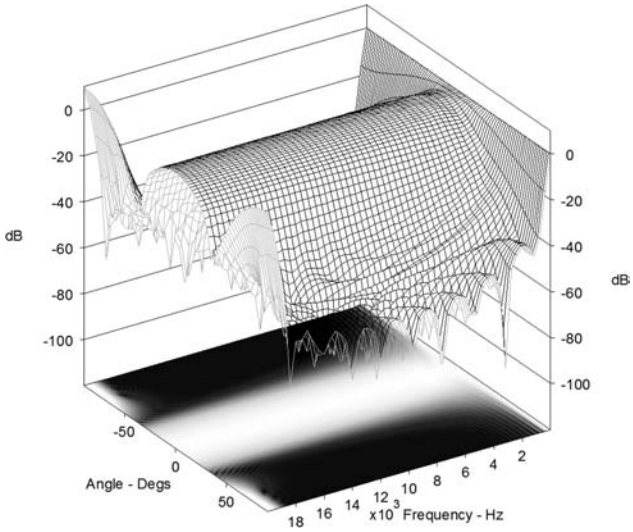

Fig. 19. Three-dimensional polar plot for constant-beamwidth curved-line CBT array with projected two-dimensional polar plot on bottom of display.

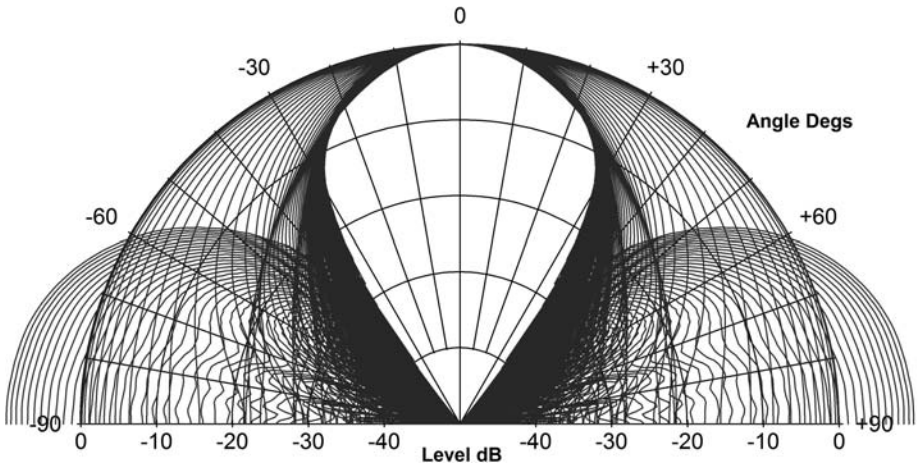

Fig. 17. Cylindrical composite polar plot for constant-beamwidth curved-line CBT array that provides a rounded-shape beam. Polar radial range is 50 dB with 10° angular increments.

(Fig. 19), the straight-line delay-curved CBT array does not provide as much off-axis attenuation. As with the previous straight-line arrays, the grating lobes appear at 10 kHz.

The magnitudes of the array coefficients of the straight-line delay-curved CBT array are identical to those of the previous CBT array (Fig. 20) and will not be repeated. Note that unlike for the previous CBT array, the coefficients are frequency dependent because of the application

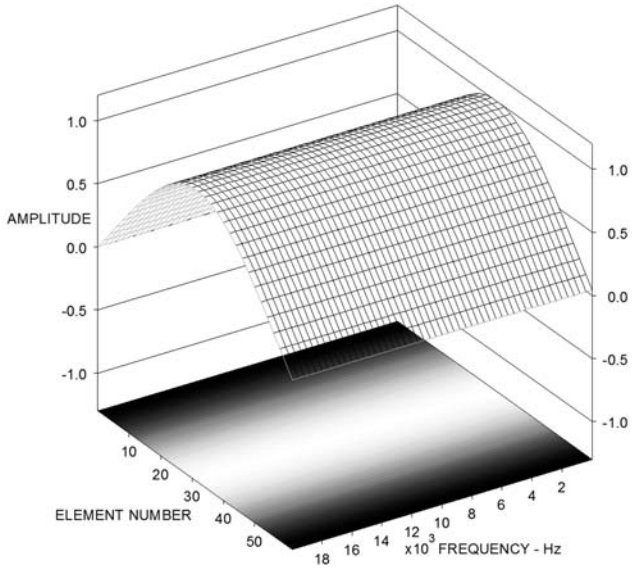

Fig. 20. Three-dimensional array coefficient plot versus frequency for constant-beamwidth curved-line CBT array. Note that plot does not include array's flat on-axis equalization and coefficients are independent of frequency.

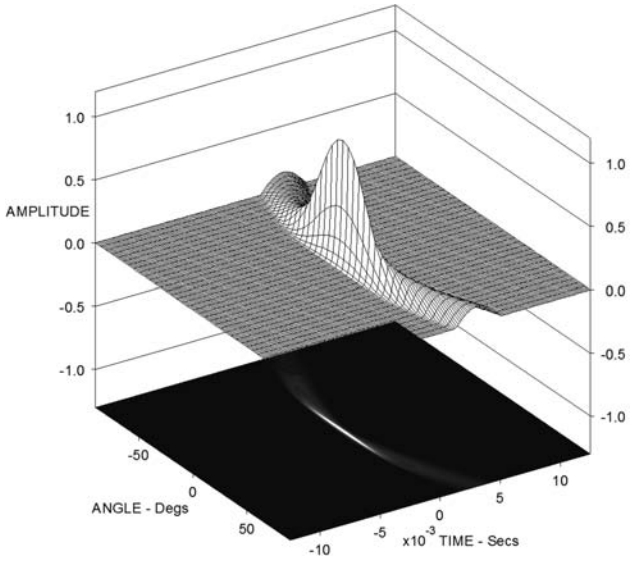

Fig. 21. Three-dimensional plot of cross correlation between on- and off-axis impulse responses for constant-beamwidth curved-line CBT array.

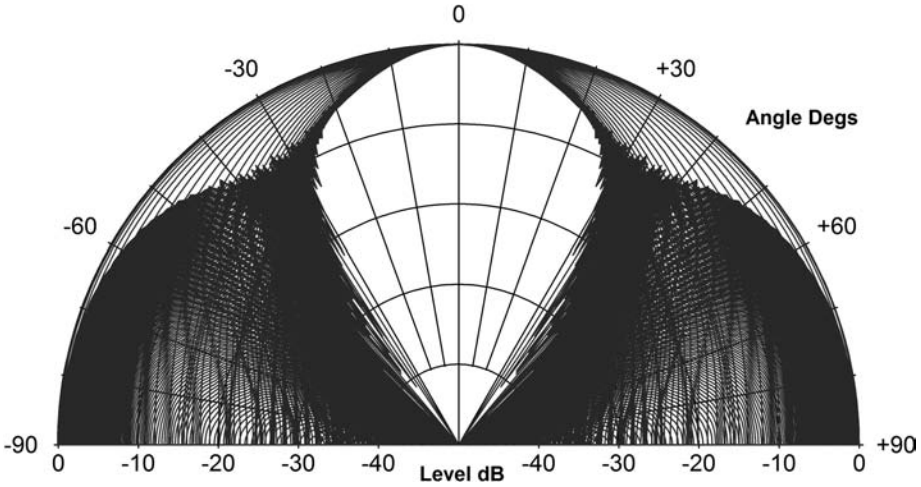

Fig. 22. Cylindrical composite polar plot for constant-beamwidth straight-line CBT array that provides a rounded-shape beam. Polar radial range is 50 dB with 10° angular increments.

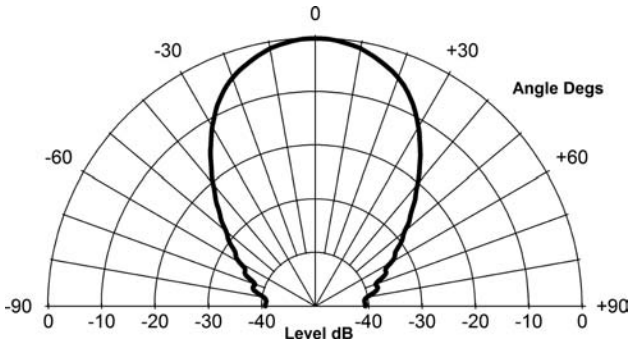

Fig. 23. Cylindrical polar plot at 6.3 kHz for constant-beamwidth straight-line CBT array that provides a rounded-shape beam.

of delays that curve the array. However, the magnitude of the array coefficients stays independent of frequency.

Fig. 25 displays the array's three-dimensional cross-correlation plot between the on- and off-axis impulse responses. This is fairly similar to the previous CBT array (Fig. 21), except that the main lobe is somewhat narrower and the skirts of the cross correlation do not curve because the array is straight.

Conclusions

I have proposed an alternate method to design constant-aperture constant-beamwidth straight-line loudspeaker arrays, which is simpler than the method proposed by Hawksford. This method takes a selected window function that sets the array's source strengths, and then scales its width with frequency using a prescribed scaling function. This scaling maintains the shape of the window as the frequency changes. I illustrated this proposed method by designing two arrays, one providing a wedge-shaped beam and the other a rounded-shape beam.

For comparison I also included simulations of two styles of a competing array, the constant-beamwidth transducer (CBT) curved- and straight-line arrays. The processing for the CBT arrays is much simpler than for the constant-aperture constant-beamwidth arrays because it is essentially independent of frequency. The CBT arrays exhibit significantly less high-frequency loss because all the array sources are driven at all frequencies. This is in contrast with the constant-aperture arrays, where only a few of the array sources are driven at high frequencies. The curved-line CBT array was shown to operate a full octave higher than straight-line arrays before high-frequency grating lobes appear due to the finite spacing of the sources.

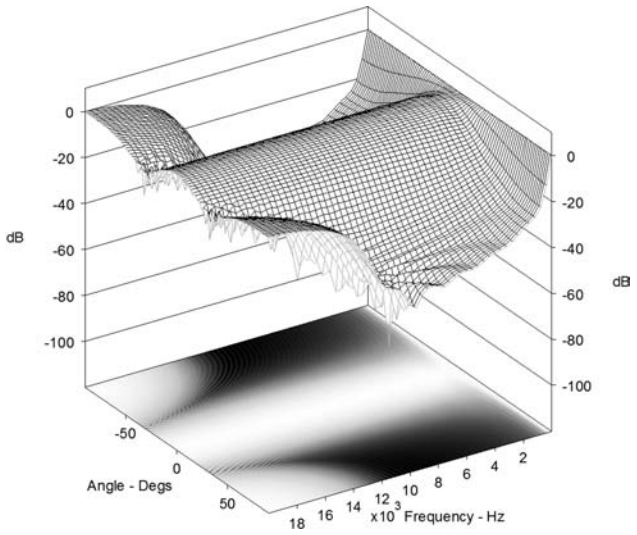

Fig. 24. Three-dimensional polar plot for constant-beamwidth straight-line CBT array with projected two-dimensional polar plot on bottom of display.

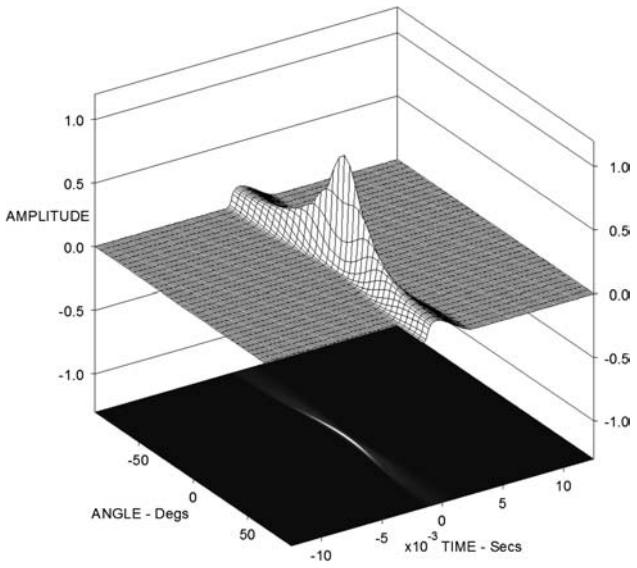

Fig. 25. Three-dimensional plot of cross correlation between on- and off-axis impulse responses for constant-beamwidth straight-line CBT array. Bottom of display shows projected two-dimensional polar plot.

ACKNOWLEDGMENT

IGOR Pro was used to simulate and plot all the graphs in this letter.[2]

REFERENCES

[1] D. L. Klepper and D. W. Steele, "Constant Directional Characteristics from a Line Source Array," *J. Audio Eng. Soc.,* vol. 11, p. 198 (1963).

[2] D. G. Meyer, "Multiple-Beam, Electronically Steered Line-Source Arrays for Sound-Reinforcement Applications," *J. Audio Eng. Soc.,* vol. 38, pp. 237–249 (1990 Apr.).

[3] D. L. Smith, "Discrete-Element Line Arrays—Their Modeling and Optimization," *J. Audio Eng. Soc., (Engineering Reports),* vol. 45, pp. 949–964 (1997 Nov.).

[4] M. van der Wal, E. W. Start, and D. de Vries, "Design of Logarithmically Spaced Constant-Directivity Transducer Arrays," *J. Audio Eng. Soc.,* vol. 44, pp. 497–507 (1996 June).

[5] P. H. Rogers and A. L. Van Buren, "New Approach to a Constant Beamwidth Transducer," *J. Acoust. Soc. Am.,* vol. 64, pp. 38–43 (1978 July).

[6] J. Jarzynski and W. J. Trott, "Array Shading for a Constant Directivity Transducer," *J. Acoust. Soc. Am.,* vol. 64, pp. 1266–1269 (1978 Nov.).

[7] A. L. Van Buren, L. D. Luker, M. D. Jevnager, and A. C. Tims, "Experimental Constant Beamwidth Transducer," *J. Acoust. Soc. Am.,* vol. 73, pp. 2200–2209 (1983 June).

[8] D. B. Keele, Jr., "The Application of Broadband Constant Beamwidth Transducer (CBT) Theory to Loudspeaker Arrays," presented at the 109th Convention of the Audio Engineering Society, *J. Audio Eng. Soc.* (*Abstracts*), vol. 48, pp. 1104, 1105 (2000 Nov.), preprint 5216.

[9] D. B. Keele, Jr., "Implementation of Straight-Line

[2] www.Wavemetrics.com

and Flat-Panel Constant Beamwidth Transducer (CBT) Loudspeaker Arrays Using Signal Delays," presented at the 113th Convention of the Audio Engineering Society, *J. Audio Eng. Soc.* (*Abstracts*), vol. 50, p. 958 (2002 Nov.), convention paper 5653.

[10] D. B. Keele, Jr., "Full-Sphere Sound Field of Constant-Beamwidth Transducer (CBT) Loudspeaker Line Arrays," *J. Audio Eng. Soc.,* vol. 51, pp. 611–624 (2003 July/Aug.).

[11] D. B. Keele, Jr., "Practical Implementation of Constant Beamwidth Transducer (CBT) Loudspeaker Circular-Arc Line Arrays," presented at the 115th Convention of the Audio Engineering Society, *J. Audio Eng. Soc.* (*Abstracts*), vol. 51, p. 1218 (2003 Dec.), convention paper 5863.

[12] F. J. Harris, "On the Use of Windows for Harmonic Analysis with the Discrete Fourier Transform," *Proc. IEEE,* vol. 66 (1978 Jan.).

D. B. (DON) KEELE, JR., *AES Fellow*
Harman International Industries
Martinsville, IN 46151